ISBN: 978-3-95450-201-1 doi:10.18429/JACoW-IBIC2018-MOPB08

EVALUATION OF THE TRANSVERSE IMPEDANCE OF PF IN-VACUUM UNDULATOR USING LOCAL ORBIT BUMP METHOD

O. A. Tanaka†, N. Nakamura, T. Obina, K. Harada, Y. Tanimoto, N. Yamamoto, K. Tsuchiya, R. Takai, R. Kato, M. Adachi,
High Energy Accelerator Research organization (KEK), 305-0801 Tsukuba, Japan

Abstract

When a beam passes through insertion devices (IDs) with narrow gap or beam ducts with small aperture, it receives a transverse kick from the impedances of those devices. This transverse kick depends on the beam transverse position and beam parameters such as the bunch length and the total bunch charge. In the orbit bump method, the transverse kick factor of an ID is estimated through the closed orbit distortion (COD) measurement at many BPMs for various beam currents [1]. In the present study, we created an orbit bump of 1 mm using four steering magnets, and then measured the COD for two cases: when the gap is opened (the gap size is 42 mm) and when the gap is closed (the gap size is 3.83 mm). The ID's kick factors obtain by these measurements are compared with those obtain by simulations and analytical evaluations.

INTRODUCTION

At KEK Photon Factory (PF) light source, we have four newly installed in-vacuum undulators (IVUs). They are located in short straight sections as shown in Fig. 1. The vacuum chambers of those IVUs have complex geometry: narrow gaps inside the undulators (the minimum gap is 3.83 mm) and tapers at the ends of undulators. Those gaps are much smaller than the typical aperture of the PF normal vacuum ducts.

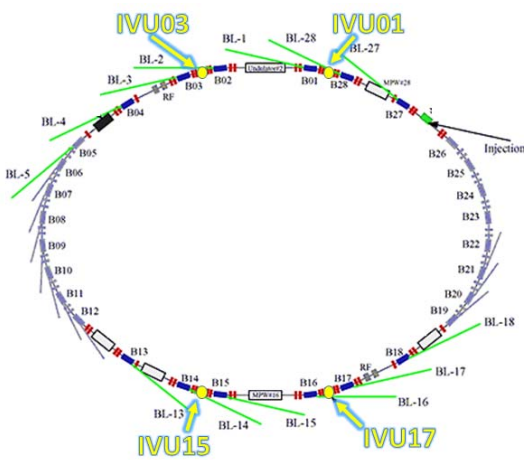

Figure 1: Locations of the IVUs in the PF ring.

First, the kick factors of the four IVUs were estimated analytically and by CST Studio simulations [2]. The total vertical kick factor due to 1 IVU including dipolar and quadrupolar kicks of the taper and resistive-wall kick of the undulator copper plates is summarized in Fig. 2.

To confirm the accuracy of the calculated transverse kick factors, we have measured the transverse tune shift with a single bunch based on the RF-KO (RF Knock Out) method [3]. The additional tune shift corresponds to a difference of the vertical tune shifts for ID open (the gap size is 42 mm) and ID closed (the gap size is 3.83 mm) cases. The result of the tune shift measurement is shown at Fig. 3. All the three evaluations demonstrated very good agreements. Thus, theory gives the tune shift value per unit of bunch current of $\Delta\nu / I_b = -10.60\times10^{-6}$ mA^{-1}. The CST Studio simulation gives those of $\Delta\nu / I_b = -10.06\times10^{-6}$ mA^{-1}. And the tune shift measurement yields the value of $\Delta\nu / I_b = -10.96\times10^{-6} \pm 1.86\times10^{-6}$ mA^{-1} including the fitting error.

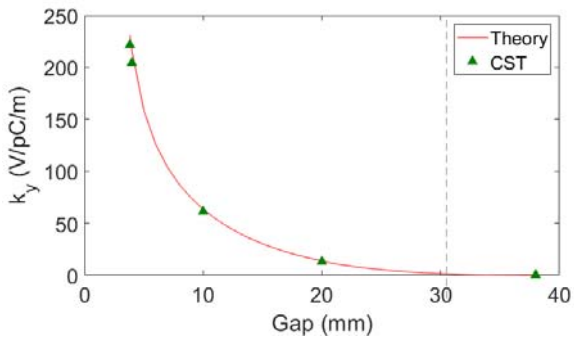

Figure 2: Total vertical kick factor due to 1 IVU (gap dependence, width fixed to 100 mm) by theory (red line), and by simulations (green triangle).

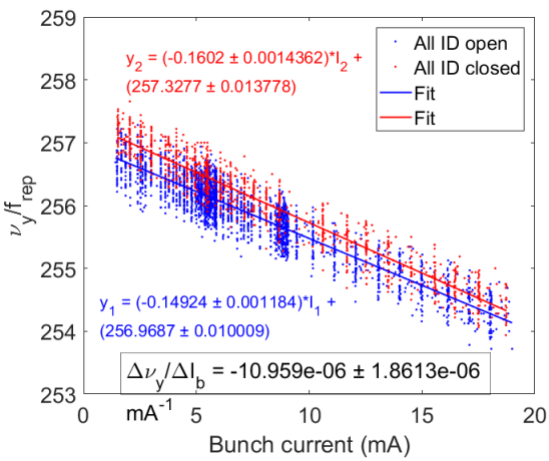

Figure 3: One of the measurement results of the additional tune shift due to the four IVU at PF.

† olga@post.kek.jp

ISBN: 978-3-95450-201-1 doi:10.18429/JACoW-IBIC2018-MOPB08

The purpose of the present study is further check of the transverse kick evaluation accuracy. To do so, we adopted the orbit bump method. We created local orbit bump at the IVU15 location and measured CODs at various BPMs for different beam currents. From these measurements, we calculated the distribution of transverse kick factors along the undulator. In the following, we show more details of these measurements.

ORBIT BUMP METHOD

The orbit bump method uses a local bump to create transverse kicks from components inside the bump. This technique was invented at Budker Institute, Novosibirsk [1]. It was successfully applied to the evaluation of the transverse impedance distribution along rings at Diamond light source [4], ESRF [5], APS [6], and many others.

The orbit bump method is found to be useful for beam ducts with considerable inhomogeneities such as flanges, ceramic breaks, bellows etc. The orbit bump generates orbit deviations at various places of the ring. Their differences for two different bunch currents are expressed by the following formula [4]:

$$\Delta y(s) = \frac{\Delta q}{E/e} k_y y_0 \frac{\sqrt{\beta(s)\beta(s_0)}}{2\sin(\pi\nu)} \cos\left[\left|\mu(s)-\mu(s_0)\right| - \pi\nu\right], \quad (1)$$

where Δq is the difference of the two bunch charges, k_y is the transverse kick factor of the ID, y_0 is the bump size, $\beta(s)$ is the betatron function at the s location. Note, that s_0 corresponds to the location of the transverse kick. The parameter $\mu(s)$ is the betatron phase advance, ν is the betatron tune, and E is the total beam energy.

We have followed the procedure outlined by V. Smaluk [4]. The first procedure is to estimate orbit deviations at all BPM locations (there are 65 BPMs at PF ring) created by the local bump of 1 mm at IVU15 location (see Fig. 1) using the analytical evaluations and CST Studio simulations of impedance of the IDs. Here, major impedance sources are the resistive-wall impedance of the 500 mm long undulator and the geometrical impedance of the 108.5 mm long tapers [2 – 3].

In Smaluk's paper, the kick factors are lumped at the center of the undulator to estimate their effects approximately. This method does not work for our case, since the beta function at the ID is very small and thus the phase advance and the beta function are changing rapidly there. Thus, we have distributed the kick factors along the ID, as shown in Fig. 4, instead of lumping the total transverse kick factor to the center of ID. This trick allows us to obtain more accurate estimate of orbit deviations at the BPMs. The kick factor due to the resistive-wall impedance, $k_{y\ R.W.} = 88.6$ V/pC/m, was uniformly distributed among 5 segments of the undulator. The kick factors of the two taper's geometrical impedance, $k_{y\ taper} = 66.5$ V/pC/m, were placed at the center of each taper (see Fig. 4). The betatron functions and the betatron phase advances at the corresponding locations were used. For an undulator of considerable length, this procedure is essential, because the phase advance will change significantly along the ID. Apparently from Eq. (1), the lumping approximation may not provide accurate estimate of orbit deviations. The values of the betatron and the betatron phase advance functions for ID15 are listed in Table 1.

The other parameters for the PF ring are: the bunch charge difference $\Delta q = 6.25$ nC, the betatron tune $\nu = 5.28$, and the total beam energy $E = 2.5$ GeV. With these parameters, we expected the maximum COD at BPM locations is $\Delta y = 1.5$ μm.

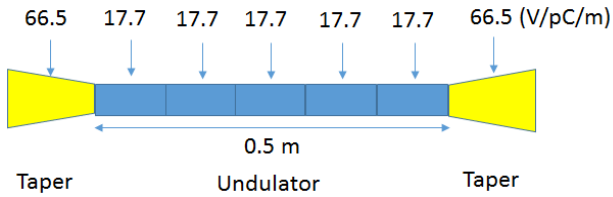

Figure 4: Transverse kick distribution along the ID.

Table 1: Betatron Functions and Betatron Phase Advances at the ID15 Locations

Position, m	Phase advance	Betatron fn, m
91.28374	14.58973	0.640564
91.41274	14.7194	0.520919
91.51274	14.89362	0.476824
91.61274	15.10334	0.47522
91.71274	15.2971	0.516108
91.81274	15.43696	0.599488
91.94174	15.53072	0.76981

MEASUREMENT

For the ID15 measurement we used the following workflow:

- Change the operation to the single bunch mode.
- Open gaps of all IDs of the ring.
- Turn the feedback off.
- Adjust the beam orbit.
- First without bump. Measure the COD at all BPM locations several times for the ID gap open/closed cases and for the beam currents of from 4 mA to 24 mA with step of 4 mA.
- Create 1 mm bump and repeat the previous step.

The parallel bump (Fig. 5) with trapezoidal shape was created using the four steering magnets: two in upstream and two in downstream of the IVU15. An example of raw measurement results is shown in Fig. 4. Here the time evolution of the 65 BPM signals is shown. The upper graph gives the x-position difference, while the middle one gives those for the y-position. The bottom graph shows the changes in the ID gap. The red zones correspond to the ID gap open case, and the blue zones correspond to those where the ID gap is closed. The intermediate zones, where the gap size was changing are excluded from the following analysis.

ISBN: 978-3-95450-201-1 doi:10.18429/JACoW-IBIC2018-MOPB08

There were slow drifts of measured beam positions. One of the possible reasons of the drift could be a time variation of the ring temperature after a user operation at 430 mA in the hybrid mode. Another concern is the position measurement resolution of the BPM, which is of the order of 1 μm. To minimize these effects on measurement results, we have picked up for the analysis several short periods close to each other, and then averaged out about a thousands of BPM data at the both red and blue zones.

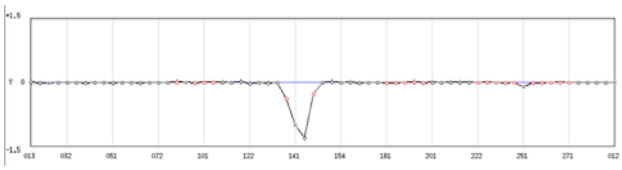

Figure 5: Orbit bump created at the ID15 location.

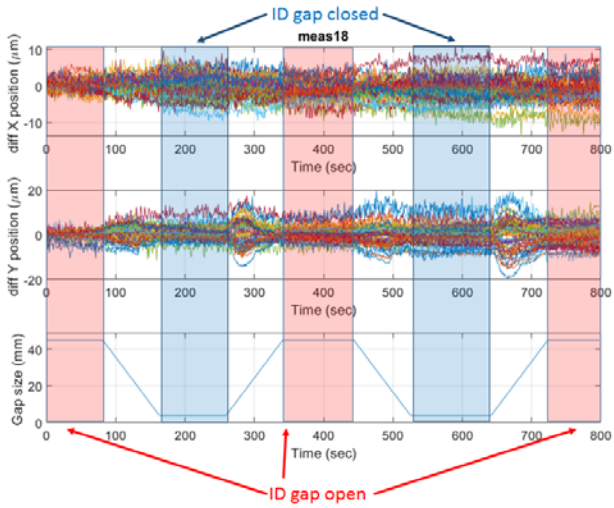

Figure 6: Example of the raw data.

DATA ANALYSIS

Taking all these considerations into account, we have analyzed the measured data. The reference [4] suggests the four-measurement combination to eliminate systematic errors by the bump itself. In this method, the difference of orbit deviation in Eq. (1) is expressed by:

$$\Delta y = (y_2 \; ? \; y_1) \; ? \; (y_{02} \; ? \; y_{01}), \tag{2}$$

where y_{01} and y_{02} are measured without the bump at the low and high values of the beam current. Then, after the bump is generated, y_1 and y_2 are measured once again at the same values of the beam current.

In the process of the analysis, we have found that this technique is not good enough for us, since the contributions to the measurements from other devices inside the same bump orbit but outside of the IDs may be significant, and we could not distinguish them from the true signals. So, we decided to take differences for the ID open and close cases:

$$\Delta y = \{(y_2 \; ? \; y_1) \; ? \; (y_{02} \; ? \; y_{01})\}|_{ID\_gap\_closed} \; ? \; \{(y_2 \; ? \; y_1) \; ? \; (y_{02} \; ? \; y_{01})\}|_{ID\_gap\_open}. \tag{3}$$

By extracting the ID open signals, we can eliminate the contributions from the extra components inside the same bump. Finally, Fig. 7 shows the measured data (based on Eq. (3) method) in red dots, while the analytical prediction based on Eq. (1) is shown in blue line. The high bunch current orbits y_2 and y_{02} corresponds to the current value of $I_b = 24$ mA, and the low current ones y_1 and y_{01} corresponds to the current of $I_b = 4$ mA. We have also evaluated the kick factors from the measurements by using the least square method. The result is shown by the green line in Fig. 7. The summary of the transverse kick factors for the ID closed case (the gap size is 3.83 mm) by the CST simulations, the analytical formulas and the measurements is presented in Table 2.

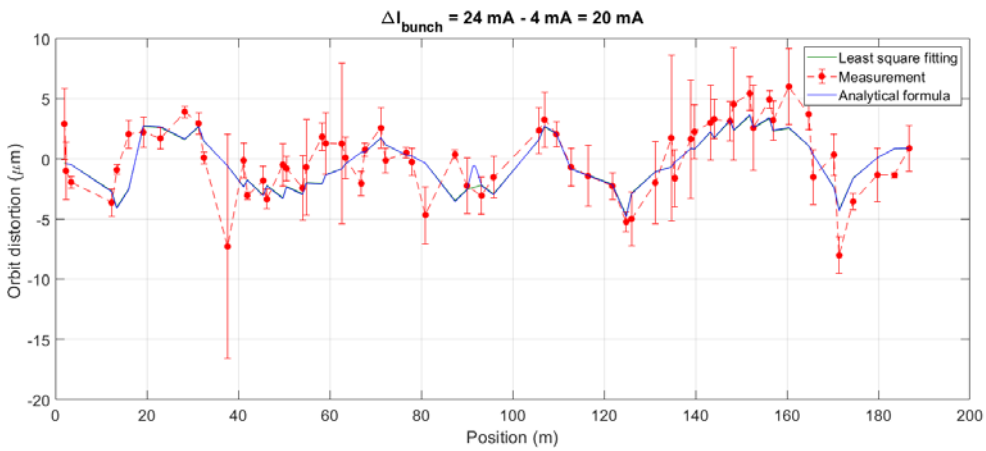

Figure 7: CODs at all the BPM locations by the measurement (red dots), by the analytical estimation (blue line), and by the least square fitting (green line).

ISBN: 978-3-95450-201-1 doi:10.18429/JACoW-IBIC2018-MOPB08

Table 2: Transverse Kick Factor Summary

	$k_{y\ R.W.}$, V/pC/m	$k_{y\ taper}$, V/pC/m
CST simulation	88.6	133.0
Analytical formula	86.1	145.4
Orbit bump measurement	91.2	135.3

CONCLUSION

We have evaluated the transverse kick factors of the PF in-vacuum undulator. The study suggests that we should distribute kick factors along the ID instead of lumping them to the center of ID for more accurate estimate of orbit deviations. Especially in the case of a long undulator this may be essential. We have also pointed out, that we should subtract contributions of other components inside the same bump orbit but outside of the undulator from analysis for more accurate estimate of kick factors. An evaluation of the impact of these "outside" components will be a natural extension of the present study. In conclusion we have compared the ID's kick factors obtained by the measurements with those obtain by the simulations and the analytical evaluations. The upcoming study will include a research on the individual properties of each of four IDs affecting the transverse kick, together with its possible reasons.

ACKNOWLEDGMENT

We would like to thank the members of PF storage ring, especially the monitor group and operational staff for their overall help.

REFERENCES

[1] V. Kiselev and V. Smaluk, *Nucl. Instrum. Methods* A, vol. 525, p. 433, 2004.

[2] O. Tanaka, N. Nakamura, T. Obina, and K. Tsuchiya, in *Proc. of 60th ICFA Advanced Beam Dynamics Workshop on Future Light Sources (FLS'18),* Shanghai, China, Mar. 4–9, 2018, pp. 160-165. doi:10.18429/JACoW-FLS2018-THP1WB02

[3] O. A. Tanaka, N. Nakamura, T. Obina, K. Tsuchiya, R. Takai, S. Sakanaka, N. Yamamoto, R. Kato and M. Adachi, *in Journal of Physics Conference Series*, to be published.

[4] V. Smaluk *et al.*, *Phys. Rev. ST Accel. Beams,* vol. 17, p. 074402, 2014.

[5] E. Karantzoulis, V. Smaluk, and L. Tosi, *Phys. Rev. ST Accel. Beams*, vol. 6, p. 030703, 2003.

[6] L Emery, G. Decker, and J. Galayda, in *Proc., 19th Particle Accelerator Conference (PAC'01)*, Chicago, IL, USA, Aug. 2001, paper TPPH070, pp. 1823-1825.